Analytical model for determination of parameters of helical structures in solution by small angle scattering: comparison of RecA structures by SANS

D.V. Lebedev[a], D.M. Baitin[a], A.Kh. Islamov[b], A.I. Kuklin[b], V.Kh. Shalguev[a], V.A. Lanzov[a], V.V. Isaev-Ivanov[a,*]

[a] *Division of Molecular and Radiation Biophysics, Petersburg Nuclear Physics Institute, Russian Academy of Sciences, Gatchina, Russia*
[b] *Frank Laboratory of Neutron Physics, Joint Institute for Nuclear Research, Dubna, Russia*

Received 14 November 2002; revised 20 December 2002; accepted 7 January 2003

First published online 7 February 2003

Edited by Thomas James

Abstract The filament structures of the self-polymers of RecA proteins from *Escherichia coli* and *Pseudomonas aeruginosa*, their complexes with ATPγS, phage M13 single-stranded DNA (ssDNA) and the tertiary complexes RecA::ATPγS::ssDNA were compared by small angle neutron scattering. A model was developed that allowed for an analytical solution for small angle scattering on a long helical filament, making it possible to obtain the helical pitch and the mean diameter of the protein filament from the scattering curves. The results suggest that the structure of the filaments formed by these two RecA proteins, and particularly their complexes with ATPγS, is conservative.

Key words: RecA protein; Small angle neutron scattering; Homologous recombination; *Pseudomonas aeruginosa*

1. Introduction

RecA protein from *Escherichia coli* is a small (~40 kDa) enzyme essential for several cellular functions such as homologous recombination, post-replication repair, recombination-dependent replication and induction of SOS-repair functions. In the presence of ATP and magnesium, these proteins polymerize on single-stranded DNA (ssDNA), forming a helical nucleoprotein filament, which is capable of binding homologous double-stranded DNA (dsDNA) and accomplishing the recombination strand exchange reaction [1]. Replacement of *E. coli recA* gene with its homolog from *Pseudomonas aeruginosa* results in hyper-recombination that is a high frequency of recombination per DNA unit length [2]. Comparative biochemical study of $RecA_{Pa}$ and $RecA_{Ec}$ proteins has revealed that the tertiary complex $RecA_{Pa}::Mg^{2+}::ATP::ssDNA$ exhibits higher stability in high salt and has a higher affinity for ssDNA and dsDNA [2,3]. It remained unclear how the differences in genetic and biochemical characteristics of the compared proteins relate to the differences in their structural parameters.

Small angle X-ray and neutron scattering are among the few methods that yield information about the structure of proteins and nucleoprotein complexes under the native condition. It has been shown earlier [4] that the scattering curve of the helical filament of *E. coli* RecA protein exhibits a distinct diffraction maximum. This maximum is attributed to the periodicity of the helix so that its position provides information on the helical pitch of the protein filament. In previous works [4] the cross-sectional radius of gyration has been determined from the Guinier region of the curve, using the approximation for very long particles [5]. The helical pitch was estimated by numerical calculation of scattering on helical objects, which were built from arrays of spheres [4] or cylinders [6], and by changing the helical pitch of such objects until the calculated curves were in agreement with the experimental data.

In this work we present a model that allows for an analytical treatment of the intensity of scattering on a long helical object in solution. Based on this model, we were able to develop a minimization routine for LMS fitting of the experimental scattering curves and to obtain such structural parameters as helical pitch, the mean diameter of the helix, and the approximate size of the protein monomer. This routine was used to compare the above parameters for the filaments of RecA proteins from *E. coli* and *P. aeruginosa* ($RecA_{Ec}$ and $RecA_{Pa}$, respectively) and their complexes with co-factors and substrates (ssDNA, ATPγS, and magnesium ions).

2. Materials and methods

2.1. Principles of the model for scattering on a helical structure in solution

The amplitude of scattering on a periodic structure oriented at an angle θ to the plane of the incident wave can be written as a convolution of two functions [7]:

$$A(Q) = \sum_{j=-\infty}^{\infty} \frac{1}{ht}\delta\left(Q-\frac{2\pi j}{ht}\right)\Psi(Q,t)\otimes Lt\frac{\sin QLt/2}{QLt/2} \quad (1)$$

where $t=\cos\theta$, h is the period of the structure, L its total length and $\Psi(Q,t)$ the form-factor of a single element of the structure ($\Psi(Q,t)=0$ at $t>1$), in this case, of one turn of the helix. Using the properties of the δ-function, Eq. 1 can be rewritten as:

$$A(Q) = \sum_{j=-\infty}^{\infty} \frac{L}{h}\frac{\sin\left(Q+\frac{2\pi j}{ht}\right)Lt/2}{\left(Q+\frac{2\pi j}{ht}\right)Lt/2}\Psi\left(\frac{2\pi j}{ht},t\right) \quad (2)$$

*Corresponding author. Fax: (7)-812-71 32303.
E-mail address: isaev@omrb.pnpi.spb.ru (V.V. Isaev-Ivanov).

Abbreviations: SANS, small angle neutron scattering; ssDNA, single-stranded DNA; dsDNA, double-stranded DNA

0014-5793/03/$22.00
doi:10.1016/S0014-5793(03)00107-8

For a sufficiently long object, so that $L \gg h$, $1/Q$, the terms in the sum in Eq. 2 are different from 0 only around $Q \approx -2\pi j/ht$. Therefore, the mean scattering intensity, averaged by orientation of the object, can be presented as:

$$I(Q) = \sum_{j=-\infty}^{\infty} \int_{-1}^{1} \left(\frac{L}{h} \frac{\sin\left(Q + \frac{2\pi j}{ht}\right) Lt/2}{\left(Q + \frac{2\pi j}{ht}\right) Lt/2} \right)^2 \left| \Psi\left(Q, \frac{2\pi j}{hQ}\right) \right|^2 \mathrm{d}t \quad (3)$$

Considering that $L \gg h$, $1/Q$, we can use the substitution:

$$u = \left(Q + \frac{2\pi j}{ht}\right) Lt/2$$

and integrate by u from $-\infty$ to $+\infty$, so that:

$$I(Q) = \sum_{j=-\infty}^{\infty} \frac{2L}{h^2 Q} \left| \Psi\left(Q, \frac{2\pi j}{hQ}\right) \right|^2 \int_{-\infty}^{\infty} \frac{\sin^2 u}{u^2} \mathrm{d}u \quad (4)$$

or

$$I(Q) = \sum_{j=-\infty}^{\infty} \frac{2\pi L}{h^2 Q} \left| \Psi\left(Q, \frac{2\pi j}{hQ}\right) \right|^2 \quad (5)$$

Thus, the scattering spectrum of a solution of long particles with periodic structure is a sum of diffraction peaks with each term different from 0 only at $Q > 2\pi|j|/h$, and includes a corresponding form-factor of a single element of the structure. To calculate the latter for a helical filament structure formed by a protein, we have assumed that each protein monomer is uniformly distributed along the helix, so that the scattering density of one turn of the helix is:

$$\rho(\vec{r}) = \frac{N}{2\pi} \int_0^{2\pi} \rho_0(\vec{r} - \vec{r}_\varphi) \mathrm{d}\varphi \quad (6)$$

where ρ_0 is the scattering density of the monomer and N is the number of monomers per turn. Then, the scattering amplitude of one helical turn is:

$$\Psi(Q) = \int_V \rho(\vec{r}) \mathrm{e}^{\mathrm{i}\vec{Q}\vec{r}} \mathrm{d}v_r \quad (7)$$

By combining Eqs. 6 and 7 we find that:

$$\Psi(Q) = \frac{N}{2\pi} \int_0^{2\pi} \Phi(Q, \theta, \varphi) \mathrm{e}^{\mathrm{i}\vec{Q}\vec{r}_\varphi} \mathrm{d}\varphi \quad (8)$$

where

$$\Phi(Q, \theta, \varphi) = \int_V \rho_0(\vec{r}) \mathrm{e}^{\mathrm{i}\vec{Q}\vec{r}} \mathrm{d}v_r$$

is the form-factor of a single protein monomer. Eq. 8 can be rewritten as:

$$\Psi(Q, \cos\theta) = \frac{N}{2\pi} \int_0^{2\pi} \Phi(Q, \theta, \varphi) \exp\left\{ \mathrm{i}Q \left(\frac{h\cos\theta}{2\pi} \varphi + \frac{D\sin\theta}{2} \cos\varphi \right) \right\} \mathrm{d}\varphi \quad (9)$$

where D is the mean diameter of the helix (Fig. 1). If we consider a simple model where the form-factor of the monomer unit is the same for all φ, Eq. 9 can be integrated analytically. As commonly used in the models of small angle scattering, the monomer can be approximated by a uniform sphere with a radius of r [8]:

$$\Phi(Q) = 3V(\rho - \rho_s) \frac{\sin(Qr) - Qr\cos(Qr)}{(Qr)^3} \quad (10)$$

Then, from Eq. 9 we obtain:

$$\left| \Psi\left(Q, \frac{2\pi j}{hQ}\right) \right| = \begin{cases} \frac{N}{2\pi} J_j \left(\frac{QD}{2} \sqrt{1 - \left(\frac{2\pi j}{hQ}\right)^2} \right) \Phi(Q), & Q \geq 2\pi|j|/h \\ 0, & Q < 2\pi|j|/h \end{cases} \quad (11)$$

where J_j are Bessel functions.

Thus, Eqs. 5, 10 and 11 give a general analytical solution for the direct problem of small angle neutron or X-ray scattering on long helical structures in solution (Fig. 1).

The earlier results indicate [4,8] that the value for the helical pitch of the nucleoprotein complexes of RecA-like proteins usually lies between 70 and 95 Å and does not exceed 100 Å. For these helical pitch values the second diffraction term (Eq. 11, $j = \pm 2$) contributes to the scattering curve only at $Q > 0.13$ Å^{-1}, which in our SANS measurements correspond to the very end of the scattering curve with poor signal-to-noise ratio. Thus, in applying Eqs. 5, 10 and 11 to our SANS data, we can disregard the terms that describe the second- and higher-order diffraction maxima and modify Eq. 11, leaving only the terms with $j = -1, 0, 1$:

$$I(Q) = \frac{NL}{h^2 Q} \left(|\Psi(Q, 0)|^2 + 2 \left| \Psi\left(Q, \frac{2\pi}{hQ}\right) \right|^2 \right) \quad (12)$$

The first term in Eq. 12 is the commonly used formula that describes scattering on lengthy particles [5], while the second term results from the periodicity of the helical structure. Eq. 12, together with Eqs. 10 and 11, were applied for LMS fitting of experimental SANS data, yielding the mean diameter of the helical structure, D, mean radius of the monomer, r, and the helical pitch of the structure, h. The cross-sectional radius of gyration was calculated as:

$$R_g^2 = 3/5r^2 + 1/4D^2 \quad (13)$$

The minimization routine was implemented in Fortran using the MINUIT library package. The fitting procedure was further tested on a set of simulated SANS scattering curves calculated for helical objects of different length and pitch, composed from an array of uniform spheres. The radius of the monomer sphere (23 Å), the mean diameter of the helix (60 Å), filament density (six monomers per turn) and the range of the helical pitch values were chosen to approximate the expected values for RecA protein [8]. The calculated scattering spectra were convoluted with the Gaussian function ($\sigma = 0.1Q$), approximating the resolution function of the YuMO spectrometer. The fitting routine used the same resolution function, while varying the parameters h, D and r. For the simulated scattering curves for objects 9000 Å in length and with helical pitch between 55 and 95 Å, the structural parameters of the filaments given by the minimization routine did not differ from the values used to generate the simulated curve by more than 2%. The simulated data could be fitted by Eq. 12 for the model objects with lengths of 3000 Å and longer, with the error in determining the parameters h, D and r not exceeding 3%. The fitting routine was unsuitable for determination of the parameters of very short (300 Å) filaments and appears to provide an adequate treatment of the scattering intensity data for the helical polymers whose length exceeds the mean diameter by at least a factor of 20–50.

2.2. Experimental procedure

SANS data were acquired on the YuMO spectrometer, Frank Laboratory of Nuclear Physics, Joint Institute for Nuclear Research in Dubna, Russia. The standard geometry was used as described in [9], with a collimated beam diameter of 14 mm. The time-of-flight method was used for the scattering curve acquisition, with the range of neutron wavelengths from 0.7 to 6 Å. The raw data were processed and normalized as described in [9], so that the absolute value (in cm^{-1}) for the scattering intensity could be determined. Two detectors were used for simultaneous acquisition in the range of Q from 0.005 to 0.15 Å^{-1}. Samples were placed in 2 mm Helma cuvettes and were maintained in a temperature-stabilized box during measurements.

RecA proteins from *E. coli* ($\mathrm{RecA_{Ec}}$) and *P. aeruginosa* ($\mathrm{RecA_{Pa}}$) were extracted and purified as described in [2], except the last dialysis was performed against D_2O buffer, and stored at 70–110 mg/ml concentration at −30°C in 50 mM Tris–HCl D_2O buffer containing 50% glycerol by volume. Protein concentrations were determined by optical absorption at 280 nm. Extinction coefficients of 2.23×10^4 M^{-1} cm^{-1} and 1.8×10^4 M^{-1} cm^{-1} were taken for $\mathrm{RecA_{Ec}}$ and $\mathrm{RecA_{Pa}}$, respectively. ssDNA from phage M13mp19 was purified as described in [10], and its concentration determined by optical absorption at 260 nm, using an extinction coefficient of 6.5×10^3 M^{-1} cm^{-1}. ATPγS, ADP, Tris, glycerol and $MgCl_2$ were from Sigma Chemical.

The measurements were performed at 15°C in >99.8% D_2O 20 mM Tris–HCl buffer (pH 7.5) containing 2 mM Mg acetate and 2–5% glycerol. A blank sample of the buffer containing the same amount of glycerol was used for reference. ATPγS (0.5 mM) and/or M13 ssDNA (six nucleotides per RecA monomer) were added at the day of the experiment with subsequent incubation for 15 min at 37°C.

RecA concentration was 6 mg/ml, except in one experiment where a concentration of 4 mg/ml was used. The acquisition time for each curve was 20–40 min. The total duration of the experiment was around 6 h. Replicate measurements, taken on each sample at the beginning and the end of the experiment, did not show significant difference in the scattering curves, indicating that the protein structure is not degraded during the time of measurements.

3. Results and discussion

3.1. Applicability of the model for treatment of SANS data for RecA protein complexes

We have further tested the fitting procedure on experimental data obtained for RecA protein from *E. coli* and its presynaptic complex with ATPγS and ssDNA. A typical scattering curve for $RecA_{Ec}$ in D_2O (>99.8%) buffer containing 2 mM Mg^{2+} is shown in Fig. 2 (squares), and the best fit to Eq. 12 is shown by the solid line. The experimental data could also be interpreted as scattering on a long hollow cylinder, according to the formula [7]:

$$I(Q) = \frac{1}{Q}\left[\frac{R_1 J_1(QR_1) - R_2 J_1(QR_2)}{Q(R_1^2 - R_2^2)}\right]^2 \quad (14)$$

where R_1 and R_2 are the outer and inner radii of the hollow cylinder and J_1 is the first-order Bessel function (Fig. 2, dotted line). However, fitting the experimental data to Eq. 14 yielded a value for the thickness of the walls of the hollow cylinder ($R_1 - R_2$) of less than 3 Å, which is much less than the size of the RecA monomer (40–60 Å). The experimental data could not be adequately described by the hollow cylinder model when a lower limit on the wall thickness of 40 Å was imposed (Fig. 2, dashed line). Therefore, it appears likely that the maximum in the scattering curve around $Q \sim 0.1$ $Å^{-1}$ is the first diffraction maximum for scattering on a long helical structure, which is reasonably well described by Eq. 12.

Fig. 3 shows scattering on the presynaptic complex of the RecA protein ($RecA_{Ec}$::Mg^{2+}::ATPγS::ssDNA), and the best fit of the data to Eqs. 12 and 14. The data show a marked shift in the position of the subsidiary maximum and decrease in the slope of the initial portion of the curve, due to structural changes of the filament as it assumes an active form.

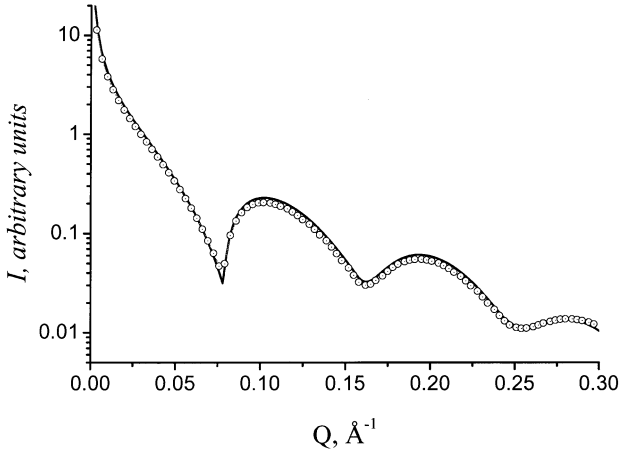

Fig. 1. Computer-simulated scattering curves on a helical structure composed from an array of uniform spheres (symbols). Helical pitch of the structure is 75 Å, mean diameter of the helix 50 Å and radius of each sphere in an array 10 Å. A curve yielded by Eq. 12 using the same parameters is shown by the solid line.

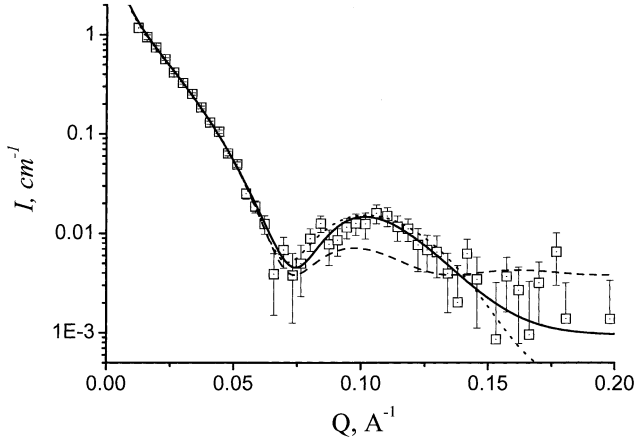

Fig. 2. SANS spectrum of RecA protein from *E. coli*, 6 mg/ml solution in Mg^{2+}-containing D_2O buffer. Solid line shows the fit to the data by Eq. 12. Fitting parameters were $D = 67.7$ Å, $h = 69.1$ Å, $r = 27.1$ Å. Data were also fitted to the hollow cylinder model (dotted line) given by Eq. 14: $R_1 = 34.4$ Å, $R_2 = 37.2$ Å. Dashed line shows an attempted fit by the latter model after a lower limit of 40 Å on the cylinder wall thickness was imposed: $R_1 = 1.6$ Å, $R_2 = 51.7$ Å, $\chi^2 = 2.25$.

Experimental points are well described by Eq. 12 (Fig. 3, solid line), which yields values for the helical pitch of 87 Å and for the mean diameter of the helix of 53 Å. The data could not be adequately described by the hollow cylinder model (Eq. 14) without any limits imposed on the wall thickness (Fig. 3, dotted line).

The earlier results obtained by SANS [4] and electron microscopy [8] have shown that $RecA_{Ec}$ forms helical filaments of two types, which correspond to the active and inactive forms of the enzyme. As summarized in Table 1, the structural parameters of the $RecA_{Ec}$ enzyme and its active complex yielded by the minimization routine based on Eq. 12 are in fairly good agreement with earlier works. Thus, the minimization routine based on Eq. 12 directly links the structural differences between the active and inactive forms of $RecA_{Ec}$ with changes in the helical pitch and the diameter of the helix. The reproducibility in the values provided by the fitting rou-

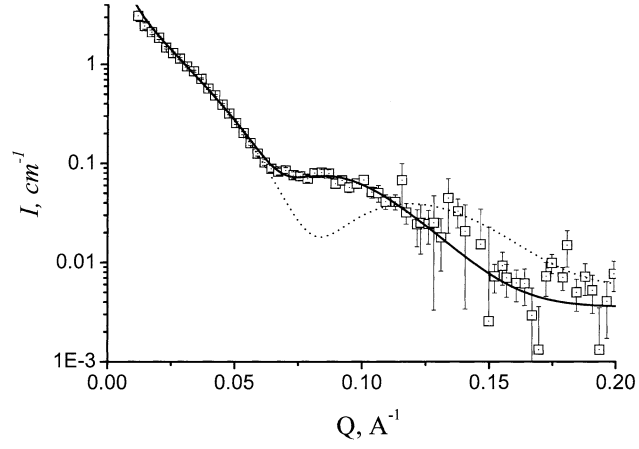

Fig. 3. SANS spectrum of *E. coli* RecA protein, 6 mg/ml solution in D_2O buffer, in the presence of ATPγS and ssDNA. Data were fitted to the helical filament model, Eq. 12 (solid line, $D = 52.6$ Å, $h = 87.2$ Å, $r = 26.6$ Å, and the hollow cylinder model, Eq. 14 (dotted line, $R_1 = 26.6$ Å, $R_2 = 34.5$ Å).

Table 1
Results of testing of the minimization routine using the SANS curves obtained for *E. coli* RecA

	Position of subsidiary maximum ($Å^{-1}$)	Helical pitch (Å)	Diameter of the helix (Å)	Monomer radius (Å)	Cross-sectional gyration radius (Å)
Inactive complex					
Present data	2π/61	69.3 ± 1.4	68.0 ± 0.6	26.2 ± 0.9	39.6 ± 0.4
DiCapua et al. [4] (SANS)	2π/63	~70	70	22.5 (estimated)	39.1 ± 1.1
Presynaptic complex					
Present data	2π/77.6	89.3 ± 2.1	53.1 ± 0.9	27.5 ± 1.4	34.1 ± 1.4
DiCapua et al. [4] (SANS)	2π/75	~95	56	22.5 (estimated)	33.5 ± 1.3
Yu et al. [8] (Image)		91			

Data are given as mean ± standard error from three independent measurements. Results reported in [4,8] are given for comparison.

tine (Table 1) indicates that it does not overinterpret the data and the fitted parameters are reasonably independent.

3.2. Comparison of the structural parameters of the protein and nucleoprotein filaments formed by $RecA_{Ec}$ and $RecA_{Pa}$

The comparative measurements of SANS spectra were performed on $RecA_{Ec}$ and $RecA_{Pa}$ complexes, such as RecA::Mg^{2+}, RecA::Mg^{2+}::ssDNA, RecA::Mg^{2+}::ATPγS and RecA::Mg^{2+}::ATPγS::ssDNA. The results of fitting the data to Eq. 12 and the obtained parameters h, D and r are summarized in Table 2. The cross-sectional radius of gyration of the filaments was calculated according to Eq. 13.

Our data indicate that in the absence of nucleotide co-factors $RecA_{Pa}$ filaments have higher helical pitch than $RecA_{Ec}$ (73.8 vs. 69.3 Å, $P < 0.05$) and somewhat lower mean diameter. In the presynaptic complex ($RecA_{Pa}$::Mg^{2+}::ATPγS::ssDNA) the helical pitch of the filament is significantly increased, which is accompanied by a decrease in filament diameter. The structural parameters of the active presynaptic complexes of the two proteins were nearly identical based on three independent measurements. The structural parameters of the complexes of these two proteins with ATPγS (RecA::Mg^{2+}::ATPγS) were also very similar. Although the latter complexes are inactive, there is a shift in the parameter values toward those for the active complex (as compared to the RecA::Mg^{2+} values). Ellouze et al. [11] have reported an even larger increase in the helical pitch of RecA protein in the presence of nucleotide co-factors, while according to the earlier work by DiCapua et al. [4] the structures of the protein self-polymer in the presence and absence of ATPγS do not appear to differ significantly. The apparent discrepancy between our data and those reported by Ellouze et al. is possibly due to somewhat different conditions of measurement, particularly the higher salt concentration (NaCl and sodium phosphate) used in that work [11], which could have resulted in a partial activation of RecA protein [12]. Our own observations seem to suggest that the helical pitch of the RecA complex with ADP::AlF_4 (an ATP analog [8]) increases substantially after addition of 200 mM NaCl (data not shown).

For the protein complexes with ssDNA alone (RecA::Mg^{2+}::ssDNA), the helical pitch values for $RecA_{Ec}$ and $RecA_{Pa}$ appear to differ, although the difference was not statistically significant due to a higher scatter in the results between different experiments under these conditions.

The high degree of similarity in the structure of the complexes of $RecA_{Pa}$ and $RecA_{Ec}$ with ATPγS and their presynaptic complexes indicates that the mechanism of the transition from the inactive to the active form of the enzyme may also be conservative. Considering the three-domain structure of RecA proteins, it may be presumed that the structural changes in the filament are accomplished by a change in the relative orientation of the domains, possibly through the existence of hinge-like structures [13]. The change in the relative orientation of the main protein domain of $RecA_{Ec}$ protein and its C-terminal domain upon binding ATPγS has been observed by fluorescent spectroscopy [14]. Reorientation of the C-terminal domain of $RecA_{Ec}$ has also been implicated in the change between the active and inactive forms of the protein by electron microscopy [8]. The changes in the helical structure of RecA proteins upon interaction with ATPγS observed in this SANS study may indicate that this nucleotide co-factor places the filament structure into an intermediate state, which is conservative between the two proteins. This intermediary, upon binding ssDNA, forms a presynaptic complex which structur-

Table 2
Structural parameters of the filaments of RecA proteins from *E. coli* and *P. aeruginosa* and their nucleoprotein complexes

Co-factor	Helical pitch, h (Å)	Mean diameter, D (Å)	Radius of the monomer, r (Å)	Cross-sectional radius of gyration, R_g (Å)	n
E. coli					
Mg^{2+}	69.3 ± 1.4	68.0 ± 0.6	26.2 ± 0.9	39.6 ± 0.4	3
ATPγS	76.9 ± 1.4[a]	66.8 ± 0.4	26.3 ± 1.7	39.1 ± 0.6	3
ssDNA	72.8 ± 2.7	65.9 ± 1.7	26.7 ± 1.0	38.9 ± 0.7	3
ATPγS::ssDNA	89.3 ± 2.1[a]	53.1 ± 1.9[a]	27.5 ± 1.4	34.1 ± 1.4[a]	3
P. aeruginosa					
Mg^{2+}	73.8 ± 1.5[b]	66.7 ± 1.0	27.1 ± 1.1	39.0 ± 0.6	3
ATPγS	77.5 ± 0.9	65.2 ± 1.6	27.3 ± 2.3	38.9 ± 0.3	2
ssDNA	77.6 ± 3.1	63.8 ± 0.6	27.6 ± 1.2	38.4 ± 0.6	3
ATPγS::ssDNA	89.6 ± 1.2[a]	50.8 ± 0.9[a]	28.3 ± 1.9	33.6 ± 0.6[a]	3

Data from independent experiments are presented as mean ± standard error.
[a]Significantly different from value for the protein self-polymer in Mg^{2+}.
[b]Significantly different from the corresponding value for *E. coli* enzyme ($P < 0.05$).

al parameters that follow the structure of a stretched conformational state of a ssDNA, as suggested in [10] and [15].

Acknowledgements: The authors are very grateful to V.A. Nazarenko (PNPI, Gatchina) and V.L. Aksenov, I.N. Serdyuk and V.I. Gordely (JINR, Dubna) for support and constant interest in the work. The authors are also thankful to M.G. Petukhov for the useful discussion on the homological modeling of three-dimentional protein structures. This work was supported by the Russian Foundation for Basic Research (Grant No. 02-04-49259), two Russian Academy of Science programs 'Neutron Physics and the Standard Model' and 'Physics of Elementary Particles', and Fogarty International Research Collaboration Award (Grant 1 R03 TWO1319-01a1).

References

[1] Kowalczykowski, S.C., Dixon, D.A., Eggelston, A.K., Lauder, S.D. and Rehrauer, W.M. (1994) Microbiol. Rev. 58, 401–465.
[2] Namsaraev, E.A., Baitin, D., Bakhlanova, I.V., Alexseyev, A.A., Ogawa, H. and Lanzov, V.A. (1998) Mol. Microbiol. 27, 727–738.
[3] Chervyakova, D., Kagansky, A., Petukhov, M. and Lanzov, V. (2001) J. Mol. Biol. 314, 923–935.
[4] DiCapua, E., Schnarr, M., Ruigrok, R.W.H., Lindner, P. and Timmins, P.A. (1990) J. Mol. Biol. 214, 557–570.
[5] Luzzati, V. (1960) Acta Crystallogr. 13, 939–945.
[6] Norden, B., Elvingson, C., Kubista, M., Sjoberg, B., Ryberg, H., Ryberg, M., Mortensen, K. and Takahashi, M. (1992) J. Mol. Biol. 226, 1175–1191.
[7] Svergun, D.I. and Fejgin, L.A. (1986) in: Rentgenovskoe i Nejtronnoe Malouglovoe Rassejanie, Nauka, Moscow, pp. 18 and 81.
[8] Yu, X., Jacobs, S.A., West, S.C., Ogawa, T. and Egelman, E.H. (2001) Proc. Natl. Acad. Sci. USA 17, 8419–8424.
[9] Ostanevich, Y.M. (1988) J. Makromol. Chem. Macromol. Symp. 15, 91–103.
[10] Shibata, T., Cunningham, R.P. and Radding, C.M. (1981) J. Biol. Chem. 256, 7557–7564.
[11] Ellouze, C., Takahashi, M., Wittung, P., Mortensen, K., Schnarr, M. and Norden, B. (1995) Eur. J. Biochem. 233, 579–583.
[12] Pugh, B.F. and Cox, M.M. (1988) J. Biol. Chem. 263, 76–83.
[13] Shatsky, M., Nussinov, R. and Wolfson, H.J. (2002) Protein Struct. Funct. Genet. 48, 242–256.
[14] Isaev-Ivanov, V.V., Kozlov, M.G., Baitin, D.M., Masui, R., Kuramitsu, S. and Lanzov, V.A. (2000) Arch. Biochem. Biophys. 376, 124–140.
[15] Xiao, J. and Singleton, S.F. (2002) J. Mol. Biol. 320, 529–558.